Proceedings of Eurodrying'2019
Torino, Italy, July 10-12, 2019

Paper 154

RESORCINOL FORMALDEHYDE HYDROGEL DRYING BEHAVIOR: DESICCATION CRACKING MODELING

***J. Hubert*[1], *A. Leonard*[1], *E. Plougonven*[2], *F. Collin*[1]**

[1]Université de Liège, Dépt. ArGEnCo
Allée de la découverte 9, 4000 Liège, Belgium
Email: julien.hubert@uliege.be
[2]Université de Liège, Dépt. Chemical Engineering
Agora Quarter, 4000 Liège, Belgium

Abstract

In this paper, we present the method used to investigate the drying behavior of the Resorcinol (R) formaldehyde (F) hydrogels and the tools needed for its numerical modeling. First, the studied material is introduced. Then the numerical model is detailed and finally convective drying simulations are performed to evaluate the capacity of our model to predict desiccation cracking.

Keywords*: Mass and heat transfer, convective drying, porous media, desiccation cracking.*

1 Introduction

Production of carbon aerogels by CO2 supercritical drying of resorcinol (R) formaldehyde (F) hydrogels followed by pyrolysis has been studied since their introduction by Pekala (Pekala, 1989). The material has been studied because its large mesopore volumes (5 cm^3/g) and high specific surface areas (500-1000 m^2/g) make it interesting for many potential industrial applications such as catalysts supports, adsorbent material, lithium-ion batteries electrodes, thermal insulation material, etc. It is an interesting alternative to activated carbon because it is a synthetic material which means its structure and properties can be accurately and reliably chosen.
In his work, he stated that the polycondensation of resorcinol with formaldehyde under alkaline conditions results in "*the formation of surface functionalized polymer clusters*". The covalent crosslinking of these clusters creates a 3D framework filled with liquid i.e. a gel. The hydrogels are dark red in color and consist of interconnected colloidal-like particles with diameters of approximately 10 nm. In this case, the hydrogel is just an intermediate phase in materials processing and Pekala used supercritical drying condition to obtain low density, organic aerogels (~<0.1g/cm^3). Supercritical drying was used because the gel would shrink or crack if the solvent was removed by evaporation. In the case of supercritical drying, no surface tension is exerted across the pores, and the dry aerogel retains the original morphology of the hydrogel.

The main limitation of the process introduced by Pekala is the supercritical drying of the hydrogel. Supercritical drying is not applicable at an industrial scale because of technical (cost) and safety reasons. Some other methods to produce an aerogel-like mesoporous texture have been tested and it has been shown (Job *et al*, 2006b) that it is possible to produce porous resorcinol–formaldehyde xerogels by using atmospheric convective drying which suppresses the main limitation of the process. Nonetheless the convective drying of the gels can, depending of the synthesis and drying conditions lead to desiccation cracking (Job, 2006). Since crack-free monoliths are required, investigating the drying behavior of the RF hydrogels is an important issue.

2 Material and method

2.1 Resorcinol formaldehyde hydrogels

It has been shown (Brunauer *et al.*, 1938) that the material properties were significantly different depending on the gel formulation and more specifically on the catalyst level. The level of catalyst is evaluated through the ratio of resorcinol (R) over catalyst (C) or R/C ratio. Job (Job, 2006) in her PhD thesis thoroughly studied the drying behavior of the resorcinol formaldehyde hydrogels. The influence of the drying air temperature and velocity were considered as well as the influence of the hydrogel formulation (R/C ratio). The convective drying experiments conducted in her PhD thesis are used throughout this work to validate our numerical model.

2.1.1 Samples preparation

Hydrogels were obtained by polycondensation of resorcinol solubilized in water with formaldehyde (resorcinol on formaldehyde ratio of 0.5) in the presence of Na_2CO_3 acting as a catalyst (C). Cylindrical samples were obtained by casting 5ml of the solution into glass molds of 22mm of diameter and putting them for curing under saturated atmosphere in an oven for 24h. For the gelation part, the solutions were placed in a water bath for 24 h at 70°C and a second cylindrical mold, slightly smaller in diameter, was slipped into the first one until it touched the solution to avoid any contact between air and the solution. Moreover, evaporation was prevented by a paraffin film covering both cylinders. This procedure aimed at avoiding thermal inertia and temperature gradients during the gelation phase. After gelation, the water content on a dry basis, W, was determined (knowing the sample initial and dry mass) and was, for all the samples, close to 2 kg/kg. R/C ratios of 300, 500 and 1000 were considered.

2.1.2 Convective drying experiment

The RF hydrogel samples were dried in a classical convective dryer controlled in air relative humidity, temperature and velocity. The samples were weighed every 10 seconds during the test. Based on the variation of the mass with time, it is possible to express the Krischer curve, representing the drying rate versus the water content. The Krischer curve used to validate our model is visible on Fig. 5 (experimental points). No other Krischer curve are presented here for clarity reasons. Nonetheless, the observations made by Job during her drying experiments are summarized hereafter.

Drying kinetics

The drying flux has been shown to increase with both temperature and air velocity. The drying fluxes for R/C ratio of 300 and 500 are very similar (with a slight decrease with increasing R/C ratio) and the drying flux for the sample prepared at R/C 1000 is much lower confirming a tendency of decreasing drying rate with increasing R/C ratio.

Cracking

During the experimental campaign, the samples produced at R/C 500 and dried at 92.5°C with an air velocity of 2m/s experienced desiccation cracking (see Fig. 1)

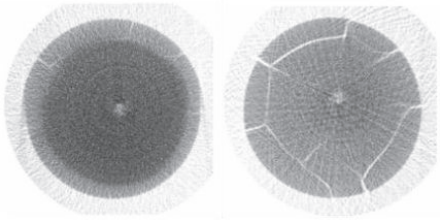

Fig. 1 : *Evolution of the desiccation cracking (W/W_0 = 0.23 on the left and W/W_0 = 0.10 on the right) (Job et al. , 2006b)*

On the scans, we see that cracking first occurs radially and then orthoradially. The samples crack radially for a length corresponding to around a quarter of their radius.

2.2 Numerical models

The process of desiccation cracking essentially results from a strain compensation mechanism. This means that, due to suction increase, shrinkage strains tend to be generated, which are hindered by a constraining mechanism (resulting from displacement or traction boundary conditions).

Such process requires a hydromechanical formulation of the problem. Furthermore, it was shown (Hubert, 2019) that temperature also plays a dominant role in the drying behavior of porous materials (even at ambient temperature drying). Thus a Thermo-Hydro-Mechanical (THM) framework is used to simulate the drying behavior of the RF hydrogels which are furthermore considered as an unsaturated porous medium with a solid phase, a liquid and gas phase.

Within that medium, the liquid water transfers are governed by Richard's equation and vapor diffusion is controlled by Fick's law. The classical heat transfer formulation is used to account for the thermal aspect of the problem. The mechanical model is an elasto-plastic constitutive law with non-linear elasticity expressed in effective stress. Finally, evaporation and heat transfer at the surface of the medium are calculated using the boundary layer model proposed by (Gerard *et al.*, 2008).

A first draft of the model has already been presented in a previous conference paper (Hubert *et al.,* 2017) but since the mechanical constitutive model has been thoroughly improved upon since and it thus detailed hereafter.

2.2.1 Water transfer

The water transfers are governed by Richard's equation:

$$\underbrace{\frac{\partial(\rho_w\, n\, S_{r,w})}{\partial t} + \frac{\partial(\rho_w q_{l,i})}{\partial x_i}}_{Liquid\ water} + \underbrace{\frac{\partial(\rho_v\, n\, S_{r,g})}{\partial t} + \frac{\partial(\rho_v q_{g,i} + i_{v,i})}{\partial x_i}}_{Water\ vapor} = Q_w \tag{1}$$

where ρ_w, ρ_v are the liquid water and the vapor densities, n is the porosity (determined experimentally based on the initial and dry mass of the sample), $S_{r,w}$ and $S_{r,g}$ are the water and gas saturation degrees in volume, t is the time, Q_w is the injected flux. $q_{l,i}$, $q_{g,i}$ are the advective fluxes of the liquid and of the gas phases with respect to the solid phase. These terms are calculated using the generalization of Darcy's law. $i_{v,i}$ is the non-advective flux (diffusion) of water vapor and is determined using Fick's law. In this work, the gas pressure is assumed to remain constant.

2.2.2 Heat transfer

The energy balance equation is :

$$\dot{S}_T + \partial \frac{V_{T,i}}{\partial\, x_i} + \dot{E}_{H_2O}^{w-v} L - Q_T = 0 \tag{2}$$

where $\dot{S}_T$ is the enthalpy of the system, $V_{T,i}$ is the heat flux, $\dot{E}_{H_2O}^{w-v}$ is the mass of water undergoing phase change from liquid water to water vapor, L is the water evaporation latent heat and Q_T is the heat production term.

2.2.3 Momentum balance equation

$$\frac{\partial \sigma_{ij}}{\partial x_j} + \rho g_i = 0 \tag{3}$$

where σ_{ij} is the total stress tensor, g_i is the gravitational acceleration vector and ρ is the density of the mixture :

$$\rho = \rho_s(1-n) + \rho_w S_{r,w} n + \rho_v\left(1 - S_{r,w}\right)n \tag{4}$$

where ρ_w, ρ_g are respectively the densities of the liquid water and water vapor.

2.2.4 Mechanical constitutive model

As mentioned, the mechanical model is an elasto-plastic constitutive law with non-linear elasticity expressed in effective stress. Effective stress is used because the strains due to drying are the consequence of a change in water content which means the use of suction as a variable of the problem is required. Non-linear elasticity is added to account for the stiffening of a material during drying (marked by a clear decrease in shrinkage rate not only explained by the decreasing saturation term in

Bishop's effective stress) stress)(Léonard *et al.*, 2008). Desiccation cracking is a mode I failure and the mechanical framework must be able to accurately deal with tensile failure. The tensile stress range allowed by a cohesive-frictional failure model is dependent on the cohesion and friction angle of the material. It has been proven (Risnes *et al.*, 1999) to lead to an overestimation of the material tensile strength. To deal with that issue, the mechanical framework is composed of two different mechanisms: a cohesive frictional failure mechanism and a tensile failure mechanism. The cohesive frictional mechanism is a Drucker-Prager criterion and the tensile failure criterion is a macroscopic Griffith like criterion.

2.2.4.1 Effective stress

Bishop's effective stress has been chosen to describe the stress-strain relation because it directly incorporates the effect of a change in suction:

$$\sigma'_{ij} = \sigma_{ij} - p_g\,\delta_{ij} + S_{r,w}\left(p_g - p_w\right)\delta_{ij} \tag{5}$$

where σ'_{ij} is the effective stress tensor, σ_{ij} is the total stress tensor, $S_{r,w}$ is the water saturation and δ_{ij} is Kronecker's tensor. p_g and p_w denote respectively gas and water pressure.

2.2.4.2 Elasto-plastic framework

As explained in the introduction, an elasto-plastic framework is required. Elasto-plasticity is based on the decomposition of the total strain increment, $d\varepsilon_{ij}$ into a reversible elastic strain increment, $d\varepsilon^e_{ij}$, and an irreversible plastic strain increment, $d\varepsilon^p_{ij}$:

$$d\varepsilon_{ij} = d\varepsilon^e_{ij} + d\varepsilon^p_{ij} \tag{6}$$

The plastic strain is said to be irreversible because it cannot be recovered even if the applied stress is removed.

Elastic strain

Hooke's law describes the relationship between the elastic strain rate, $\dot{\varepsilon}^e_{ij}$, and the effective stress tensor, $\dot{\sigma}'_{ij}$:

$$\dot{\sigma}'_{ij} = C^e_{ijkl}\;\dot{\varepsilon}^e_{ij} \tag{7}$$

where C^e_{ijkl} is Hooke's elastic constitutive tangent tensor. A material subjected to a decrease in water content tends to stiffen and thus non-linear elasticity is used in this framework. The formulation used is:

$$E = E_0 + \Delta E_{max}\left(1 - \left(1 + \left(\frac{s}{a}\right)^b\right)^{-\left(1-\frac{1}{b}\right)}\right) \tag{8}$$

where E_0 is the initial value of the Young modulus, ΔE_{max} is the maximum increase in Young modulus, s is the suction and a and b are model parameters. This formulation is a modification of the expression proposed by (Cajuhi, 2018).

Plastic strain

Most soil mechanics elasto-plastic constitutive frameworks are based on the concept of yield criterion. When the stress path reaches the yield limit, the material adopts a plastic behavior. Since we have two independent plastic mechanisms, the total plastic strain increment is the sum of two plastic strain increments (a cohesive frictional failure mechanism (p_1) and a tensile failure mechanism (p_2)) :

$$d\varepsilon^p_{ij} = d\varepsilon^{p\,1}_{ij} + d\varepsilon^{p\,2}_{ij} \tag{9}$$

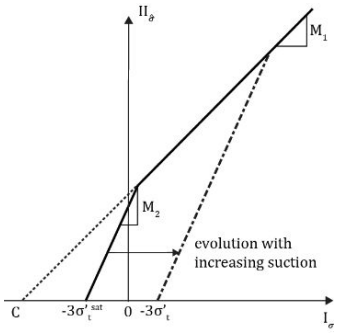

Fig. 2 : *Yield surfaces in the invariant plane*

Cohesive frictional failure mechanism

Shear failure is most often represented using a cohesive frictional failure criterion. The criterion chosen is the Drucker-Prager one, expressed in the invariant plane (see Fig. 2) by:

$$f^1 \equiv II_{\hat{\sigma}} - M_1(I_\sigma + C) = 0 \tag{10}$$

where $M_1 = \frac{2sin\phi}{\sqrt{3}(3-sin\phi)}$, $C = \frac{3c}{\tan\phi}$ with c being the cohesion and ϕ the friction angle. I_σ, $II_{\hat{\sigma}}$ represent respectively the first invariant of the stress tensor and the second invariant of the deviatoric stress tensor.

Tensile failure criterion

As already mentioned, we propose to adopt a macroscopic Griffith like criterion for tensile failure. It assumes the existence of a tension cut-off. Similar hypothesis are common in tensile failure modeling. The failure occurs when the minor principal effective stress reaches the effective tensile strength of the material $\sigma'_3 = \sigma'_t$. This is the cut off criterion as it is introduced in the work of Morris (Morris *et al*, 1992) but expressed in effective stress. It is expressed, in terms of stress invariant as (see Fig. 2) :

$$f^2 \equiv II_{\hat{\sigma}} + M_2(I_\sigma + 3\sigma'_t) = 0 \tag{11}$$

Where $M_2 = \frac{1}{-3\,cos\beta - \sqrt{3}\,sin\beta}$, β is Lode angle and σ'_t is the effective tensile strength of the material. The effective tensile strength is used because experimental evidences (Péron, 2008) have shown that the tensile strength of materials depends on suction and the model must include that feature. The formulation suggested by Péron is used to describe the evolution of the tensile strength with suction (see Fig. 3) :

$$\sigma'_t = \sigma'^{sat}_t - k_2\left[1 - exp\left(-\frac{k_1\, s}{k_{2,0}}\right)\right] \tag{12}$$

where σ'^{sat}_t is the effective tensile strength at the saturated state (s = 0), k_1 and k_2 are material parameters accounting for the increase in tensile strength as suction increases. k_2 has the dimension of a stress, and k_1 has no dimension. k_2 is the variation of tensile strength from the saturated state, σ'^{sat}_t, to the dried state, σ'^{f}_t :

$$k_2 = \sigma'^{sat}_t - \sigma'^{f}_t \tag{13}$$

This model means that the *effective* tensile strength may lie in the negative range due to the contribution of the suction. This allows for the activation of the tensile strength criterion at high suction levels.

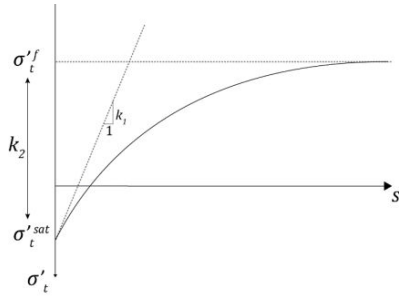

Fig. 3 : *Formulation suggested by Péron (Péron, 2008)*

2.2.4.3 Boundary layer model – vapor and heat exchange

The model is based on the assumption of the existence of a boundary layer all around the sample where the mass and heat transfers are assumed to take place (Kowalski, 2012). The water flow, $\bar{q}$, from the materials to the surroundings is assumed to be proportional to the difference between the vapor density of the drying fluid, $\rho_{v,air}$, and at the surface of the sample, $\rho_{v,surf}$, (Gerard *et al.,* 2008). The proportionality coefficient is a mass transfer coefficient, $\alpha\left(S_{r,w}\right)$, characterizing the surface transfer properties. The mass transfer coefficient is dependent on the saturation degree of the surface of the sample because it is assumed that the saturation degree of the boundary layer is equivalent to the one at the surface of the sample. As the saturation of the boundary layer decreases the transfer coefficient decreases too. The water flow is expressed as:

$$\bar{q} = \alpha\left(S_{r,w}\right)\left(\rho_{v,surf} - \rho_{v,air}\right) \tag{14}$$

The heat flux , $\bar{f}$, from the boundary to the drying air is expressed as:

$$\bar{f} = L\bar{q} - \beta_T\left(T_{air} - T_{surf}\right) \tag{15}$$

where T_{air} is the temperature of the drying air, T_{surf} is the temperature at the surface of the sample, β_T is a heat transfer coefficient and L is water evaporation latent heat. The value of the drying rate during the CRP is directly linked to capacity of the drying air to evaporate the water at the surface of the porous medium and is thus linked to the value of the mass transfer coefficient. Hence, to determine the value of the transfer coefficient, the value of the drying rate during the constant rate period (CRP) is used. Same can be said of the heat transfer: during the CRP, the temperature corresponds to the wet bulb temperature which can be analytically determined. So, no measurements of the temperature are required and only knowing the drying rate is enough to determine the heat transfer coefficient. From the experiments of Job (Job *et al.*, 2006b), we get the following values (Table 1):

Table 1 : Mass and heat transfer coefficients

Parameter	Value	Units
α	0.061	[m/s]
β	50.70	[W/m²/K]

3 Results

In this section, the numerical simulations performed using the THM model are presented. To this end, the finite element code LAGAMINE developed at the University of Liege (Collin *et al.*, 2002) in which the previously presented model was implemented is used. The goal of the simulations is to predict desiccation cracking of resorcinol formaldehyde hydrogel samples. We try to reproduce the behavior of one of the samples dried by Job (Job, 2006b). We arbitrarily chose to simulate a sample of R/C 500 dried at 92.5°C with air velocity of 2m/s because it experienced desiccation cracking. The sample is a cylinder of height 10 mm and of radius 12.5 mm. The sample was dried laterally in a classical convective drier.

3.1 Mesh, initial and boundary conditions

The simulations are performed in axisymmetric conditions given the cylindrical shape of the sample. We decided to consider a 2 mm high band in the middle of the sample. This possible because the material is homogeneous and isotropic allowing us to use the symmetry of the geometry to reduce the problem to a 1D axisymmetric configuration.

The vertical displacements at the bottom of the sample are prevented as well as horizontal displacements along the symmetry axis. The atmospheric pressure is applied at all the external boundaries. The boundary layer boundary condition is implemented through a water pressure and a temperature at the environmental node and is imposed on the lateral surface of the sample. The temperature imposed corresponds to the temperature of the drying air (i.e. 92.5°C) and the water pressure is calculated based on the temperature and relative humidity (1.5 %) using Kelvin's Law :

$$p_c = -\frac{\rho_w\, R\, T}{M}\ln(RH) = 711.9\ [MPa] \tag{16}$$

where ρ_w is the water density, R is the gas constant, M is the water molar mass and T and RH are the temperature and relative humidity of the drying air. The mesh and boundary conditions are visible on

Fig. 4. The number of elements is progressively increased towards the drying surface since this is where all the stress and water content gradients will occur. The sample is initially at rest, saturated and at room temperature.

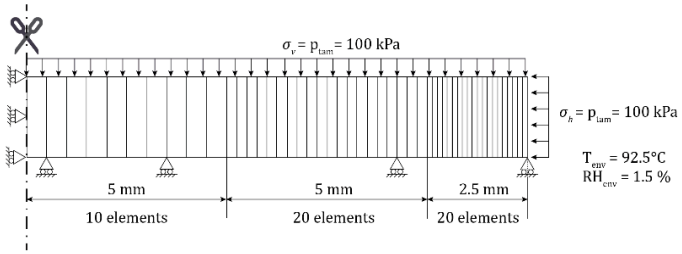

Fig. 4 : *Mesh, initial and boundary conditions*

3.2 Numerical results

Using the THM framework described before, the following (Fig. 5) Krischer curve can be obtained :

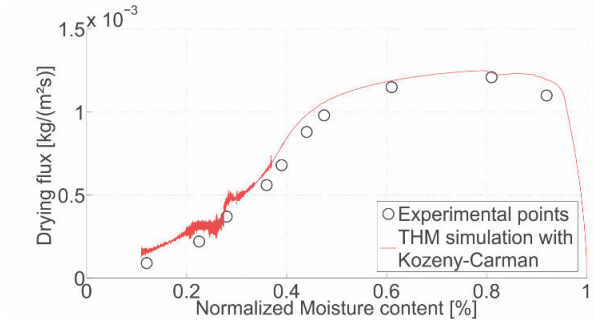

Fig. 5 : *Krischer's curve comparing RF hydrogels numerical and experimental drying kinetics*

As shown on Fig.5, there is a very good correspondence between experimental and numerical results. Such and accurate result can only be obtained through the use of a multi-physics coupled model. A step by step approach highlighting the influence of each additional mechanisms can be found in Hubert (Hubert, 2019). The drying aspect of the problem is accurately reproduced but the goal is to predict desiccation cracking. To verify if the sample cracks, we draw the evolution of the effective minor principal stress, σ_3', (which is, in this configuration, the orthoradial stress) with time as well as the evolution of the effective tensile strength of the material, σ_t', with time. If those curves touches, it will mean that the sample the tensile failure criterion is reached and that the sample has cracked. Fig. 6 presents these evolutions at the surface of the sample. It is clearly seen that the tensile failure criterion is verified leading to the onset of a radial crack starting at the surface of the sample.

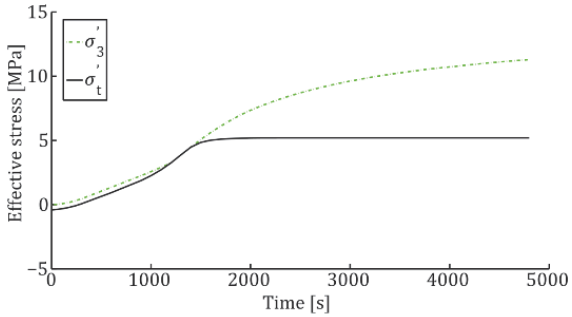

Fig. 6 : *Evolution of the effectives stresses with time at the drying surface of the sample*

Looking further inside will allow us to determine the crack propagation length. To get a better assessment of the crack length we look at the evolution of the plastic strain (generated only where the criterion is met) along the radius of the sample (see Fig. 7).

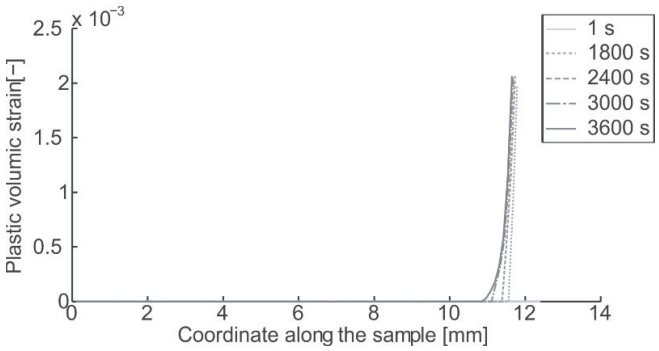

Fig. 7 : *Evolution of the plastic strain along the radius of the sample at different time steps.*

On this graph, it is clear that the crack propagated for a length of a bit less than 1mm but not more than that. This cracking means that the sample cracks for around 8 % of its radius which is lower than what was experimentally observed.

4 Conclusions

In this paper, we presented a numerical model to simulate the drying behaviour of porous material and to predict desiccation cracks onset. The studied material has been introduced and its drying behavior has been briefly described through the work of Job (Job, 2006). Then the full set of governing equations used in our THM coupled model has been presented. Those equations have been implemented into the finite element code LAGAMINE developed at the University of Liege and numerical simulations have been performed to reproduce the drying behavior of a sample of Resorcinol-Formaldehyde. The results of the simulations have proven the capacity of the model to accurately reproduce the drying behavior of the material as well as predicting desiccation cracking initiation. The post cracking behavior is not addressed in this work and requires further developments.

5 References

Brunauer, S., Emmett, P. H., Teller, E., 1938. Adsorption of gases in multimolecular layers. Journal of the American chemical society 60 (2), 309–319.

Cajuhi, T., Sanavia, L., De Lorenzis, L., 2018. Phase-field modeling of fracture in variably saturated porous media. Computational Mechanics 61 (3), 299–318.

Collin, F., Li, X.-L., Radu, J.-P., Charlier, R., 2002b. Thermo-hydro-mechanical coupling inclay barriers. Engineering Geology 64 (2), 179–193.

Gerard, P., Charlier, R., Chambon, R., Collin, F., 2008. Influence of evaporation and seepage on the convergence of a ventilated cavity. Water resources research 44 (5).

Hubert, J., Plougonven, E., Léonard, A. and Collin, F., 2017. Study of the Drying Behavior of Resorcinol Formaldehyde Hydrogels: Experimental Investigation and Numerical Framework. Proceedings of the 6th Biot Conference on Poromechanics, 473-480.

Hubert, J., 2019. Experimental and numerical study of cracking during the drying of porous materials: application to the fields of chemical engineering and geomechanics, PhD thesis, Liege University (Belgium).

Job, N., 2006. Matériaux carbonés poreux de texture contrôlée synthétisés par procédé sol–gel et leur utilisation en catalyse hétérogène., PhD thesis, Liege University (Belgium).

Job, N., Sabatier, F., Pirard, J.-P., Crine, M., Léonard, A., 2006b. Towards the production of carbon xerogel monoliths by optimizing convective drying conditions. Carbon 44 (12), 2534–2542.

Kowalski, S. J., 2012. Thermomechanics of drying processes. Vol. 8. Springer Science & Business Media.

Morris, P. H., Graham, J., Williams, D. J., 1992. Cracking in drying soils. Canadian Geotechnical Journal 29 (2), 263–277.

Léonard, A., Blacher, S., Crine, M., Jomaa, W., 2008. Evolution of mechanical properties and final textural properties of resorcinol–formaldehyde xerogels during ambient air drying. Journal of Non-Crystalline Solids 354 (10-11), 831–838.

Pekala, R., 1989. Organic aerogels from the polycondensation of resorcinol with formaldehyde. Journal of materials science 24 (9), 3221–3227.

Péron, H., 2008. Desiccation cracking of soils. Ph.D. thesis, École Polytechnique Fédérale de Lausanne, Suisse.

Risnes, R., Korsnes, R., Vatne, T., et al., 1999. Tensional strength of soft chalks measured in direct and brazilian tests. In: 9th ISRM Congress. International Society for Rock Mechanics.